



Available online at <http://scik.org>

J. Math. Comput. Sci. 11 (2021), No. 2, 1413-1436

<https://doi.org/10.28919/jmcs/5300>

ISSN: 1927-5307

A MATHEMATICAL STUDY ON ENTROPY ANALYSIS IN MHD FORCED CONVECTIVE FLOW THROUGH A CIRCULAR CHANNEL

M. JEYARAMAN^{1,*}, L. SAHAYA AMALRAJ^{2,†}, V. ANANTHASWAMY³

¹P.G. and Research Department of Mathematics, Raja Doraisingam Govt. Arts College, Sivagangai,

Affiliated to Alagappa University, Karaikudi, Tamil Nadu, India

²P.G. and Research Department of Mathematics, Raja Doraisingam

Govt. Arts College, Sivagangai. Affiliated to Alagappa University, Karaikudi, Tamil Nadu, India

³Research Centre and PG Department of Mathematics, The Madura College, Madurai, Tamil Nadu, India

Copyright © 2021 the author(s). This is an open access article distributed under the Creative Commons Attribution License, which permits unrestricted use, distribution, and reproduction in any medium, provided the original work is properly cited.

Abstract: In this paper, we study the effect of the flow of a viscous incompressible fluid within a circular channel filled with a hyper porous medium saturated with a rarefied gas amid a transverse magnetic field, thermal radiation and uniform heat flux on the walls. The velocity and heat equations of the fluid flow are solved analytically using the Homotopy Analysis Method (HAM). Approximate analytical expressions are determined for the velocity and temperature profiles and these profiles together with the entropy generation rate are discussed graphically. The results are compared with the previous study and found to be in consensus.

Keywords: forced convection; hyper porous medium; MHD; radiation; homotopy analysis method.

2010 AMS Subject Classification: 34A34, 92B05, 93C10.

*Corresponding author

E-mail address: jeyaraman.maths@rdgacollege.in

†Part-time Ph.D Research Scholar

Received December 04, 2020

1. INTRODUCTION

Entropy is a measure of randomness or molecular disorder of a system. As this randomness increases, the entropy becomes larger. A process for which the rate of entropy generation is always zero is a reversible process. The second law of thermodynamics states that the entropy generation rate within a system is greater than or equal to zero, and it can never decrease over time. All real processes are therefore irreversible. Entropy generation play important roles in many diverse areas like the global energy, the fluid flow systems, the mechanical and chemical engineering and they form the basis of equilibrium and non-equilibrium thermodynamics. Bejan ([2] - [4]) studied the impact of irreversibility due to heat transfer and that of viscous effects. Ways are formulated to minimize the irreversibility related to a specific convective heat transfer process . Minimization of entropy generation rate and second law analysis on heat transfer have been discussed. Ahmed and Das [5] analyzed the effects of heat and mass transfer of an oscillatory convective magnetohydrodynamic(MHD) channel flow of an electrically conducting viscous incompressible fluid. It is observed that the primary fluid flow has a retarding effect due to angular velocity of the system. Pakdemirli and Yilbas [6] investigated the entropy generation of a non-Newtonian third-grade fluid flow in a pipe system and concluded that the non-Newtonian parameter reduces the fluid friction. Bouchoucha and Bessiah [7] studied the natural convection and entropy generation of nanofluids in a square cavity and concluded that the maximum total entropy generation rate is attained at a low Rayleigh number. Loganathan and Sivapoornapriya [8] investigated the heat and mass transfer effects on a natural convective flow over an impulsively started vertical plate in the presence of a porous medium and concluded that the concentration boundary layer decreases as the Schmidt number increases. In[9],[13]we find analysis of the effects of MHD force and buoyancy on convective heat and mass transfer flow past a moving vertical porous plate in the presence of thermal radiation and chemical reaction and it is asserted that the velocity and temperature profiles increase with the thermal radiation.[10], [11]concluded that the entropy generation is inversely proportional to the magnetic field by investigating its variation due to mixed

convection between two isothermal cylinders with a transverse magnetic field applied on it and with the increase in radius ratio, the entropy generation induced by MHD flow also increases. Ananthaswamy et.al [12] obtained analytical solutions for velocity, temperature and concentration profiles for the boundary layer flow of a nanofluid.

The objective of this paper is to study the effect of an MHD forced convective flow of a fluid through a circular duct filled with a permeable medium concentrated with a low density gas in the presence of transverse magnetic field, thermal radiation and uniform heat flux at the walls of the duct. The velocity and temperature profiles are obtained by using the Homotopy Analysis Method (HAM) ([14]-[19]) and using them the entropy generation rate, the Bejan number and Nusselt number are determined.

2. MATHEMATICAL FORMULATION OF THE PROBLEM

We consider the steady flow of a viscous incompressible electrically conducting fluid through the \bar{x} direction, which is taken as the axis of the circular channel. A uniform magnetic field is applied in the transverse direction of the channel. The schematic diagram of the problem is shown in Fig.1. [1]

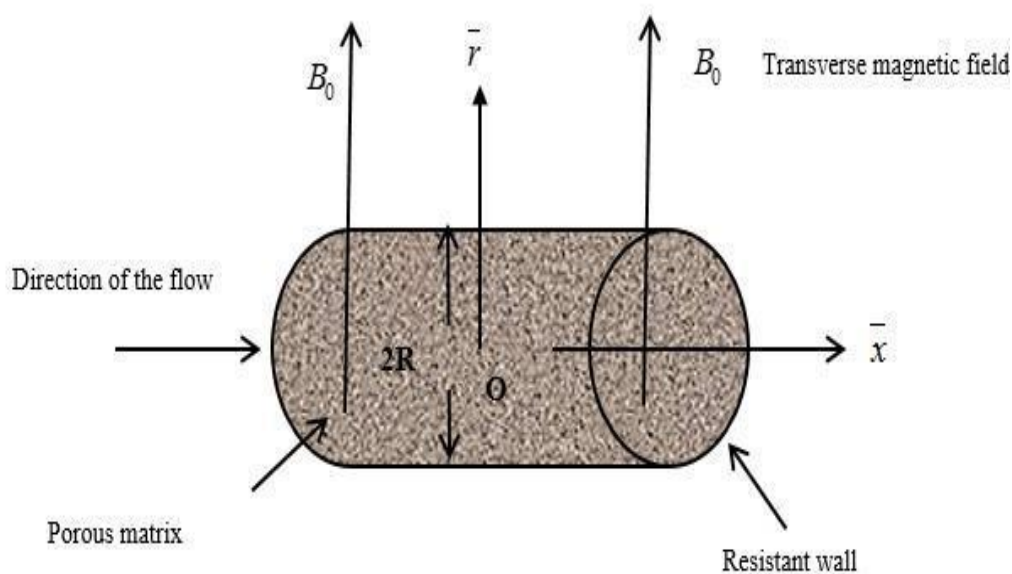


Fig.1: Schematic diagram of the problem

The internal part of the circular channel is filled with a hyper porous medium concentrated with rarefied gas. It is assumed that the wall of the circular channel is impermeable and the radiation heat flux in the \bar{x} direction is negligible. The governing equations of the fluid flow are given below.

$$\mu_{\text{eff}} \left(\frac{d^2 \bar{u}}{dr^2} + \frac{1}{r} \frac{d\bar{u}}{dr} \right) - \frac{\mu}{K} \bar{u} - \sigma B_0^2 \bar{u} - \frac{C_1 \rho \bar{u}^2}{\sqrt{K}} + P = 0 \quad (1)$$

$$\rho C_p \bar{u} \frac{d\bar{T}}{dx} = \frac{\kappa}{r} \frac{\partial}{\partial r} \left(r \frac{d\bar{T}}{dr} \right) + \frac{\mu}{K} \bar{u}^2 + \mu_{\text{eff}} \left(\frac{d\bar{u}}{dr} \right)^2 + \sigma B_0^2 \bar{u}^2 - \frac{1}{r} \frac{\partial}{\partial r} (r q_r) \quad (2)$$

The corresponding boundary conditions are as follows:

$$\begin{aligned} \bar{r} = 0: \quad \frac{d\bar{u}}{dr} = 0, \quad \frac{d\bar{T}}{dr} = 0, \\ \bar{r} = R: \quad \bar{u} = -\bar{\alpha} \frac{d\bar{u}}{dr}, \quad \bar{T} = -\bar{\beta} \frac{d\bar{T}}{dr}. \end{aligned} \quad (3)$$

Following the Roseland approximation the radiative heat flux q_r is given by

$$q_r = -\frac{4\sigma}{3\phi} \frac{\partial \bar{T}^4}{\partial r}. \quad (4)$$

The Taylor series for \bar{T}^4 about \bar{T}_w after neglecting the higher order terms, is given as

$$\bar{T}^4 \cong 4\bar{T}_w^3 \bar{T} - 3\bar{T}_w^4. \quad (5)$$

Using the eqns.(4) and (5) in an eqn. (2), we get

$$\rho C_p \bar{u} \left(\frac{\partial \bar{T}}{\partial x} \right) = \left(\kappa + \frac{16\sigma \bar{T}_w^3}{3\phi} \right) \left\{ \frac{\partial^2 \bar{T}}{\partial r^2} + \frac{1}{r} \frac{\partial \bar{T}}{\partial r} \right\} + \frac{\mu}{K} \bar{u}^2 + \mu_{\text{eff}} \left(\frac{\partial \bar{u}}{\partial r} \right)^2 + \sigma B_0^2 \bar{u}^2 \quad (6)$$

We now introduce the following dimensionless quantities

$$\begin{aligned} z = \frac{\bar{z}}{PeR}, \quad r = \frac{\bar{r}}{R}, \quad u = \frac{\mu \bar{u}}{PR^2}, \quad \mu_1 = \frac{\mu_{\text{eff}}}{\mu}, \quad Da = \frac{\bar{K}}{R^2}, \quad \eta = \sqrt{\frac{1}{Da}}, \quad F = \frac{\rho C_i PR^3}{\mu^2}, \quad Pe = \frac{\rho C_p R \bar{U}_{\text{mean}}}{\kappa}, \\ \alpha = \frac{\bar{\alpha}}{R}, \quad \beta = \frac{\bar{\beta}}{R}, \quad M = \sqrt{\frac{\sigma B_0^2 R^2}{\mu}}. \end{aligned} \quad (7)$$

Using the eqn.(7), the eqn. (1) is reduced in dimensionless form

$$\frac{d^2 u}{dr^2} + \frac{1}{r} \frac{du}{dr} - \frac{\eta^2}{M} u - \frac{M^2}{\mu_1} u - \frac{F\eta}{\mu_1} + \frac{1}{\mu_1} = 0 \quad (8)$$

The corresponding boundary conditions for velocity field are given by

$$r = 0: \frac{du}{dr} = 0, \quad r = 1: u = -\alpha \frac{du}{dr}. \quad (9)$$

The mean velocity \bar{U}_{mean} and bulk mean temperature \bar{T}_{mean} are given as

$$\bar{U}_{mean} = \frac{2}{R^2} \int_0^R \bar{u} \bar{r} d\bar{r} \quad \text{and} \quad \bar{T}_{mean} = \frac{2}{R^2 \bar{U}} \int_0^R \bar{u} \bar{T} \bar{r} d\bar{r} \quad (10)$$

We use the following dimensionless variables:

$$u = \frac{\bar{u}}{\bar{U}_{mean}}, \quad T = \frac{\bar{T} - \bar{T}_w}{\bar{T}_{mean} - \bar{T}_w}, \quad Nu = \frac{2Rq_w}{\kappa(\bar{T}_w - \bar{T}_{mean})}, \quad (11)$$

From the first law of thermodynamics, for uniform heat flux on the wall, we have

$$\frac{\partial \bar{T}}{\partial x} = \frac{2q_w}{\rho C_p R \bar{U}_{mean}}. \quad (12)$$

Now using the eqns.(11) and (12), the eqn.(6) can be reduced as follows:

$$\frac{d^2 T}{dr^2} + \frac{1}{r} \frac{dT}{dr} + (Nu)uL + \eta^2 Bru^2L + Br\mu_R L \left(\frac{du}{dr} \right)^2 + M^2 Bru^2L = 0. \quad (13)$$

Where $Br = \frac{\mu \bar{U}_{mean}^2}{\kappa(\bar{T}_{mean} - \bar{T}_w)}$ is the Brinkmann number, $N = \frac{\kappa \phi}{4\sigma \bar{T}_w^3}$ the Radiation parameter and

$L = \frac{3N}{3N+4}$. The corresponding boundary conditions for temperature field are:

$$r = 0: \frac{dT}{dr} = 0, \quad r = 1: T = -\beta \frac{dT}{dr}. \quad (14)$$

The Nusselt number can be found by substituting u and T in the compatibility condition

$$\int_0^1 u T r dr = \frac{1}{2} \quad (15)$$

The entropy generation coefficient is given as

$$N_s = Ns_1 + Ns_2 + Ns_3 \quad (16)$$

where entropy generation due to heat transfer is given by

$$Ns_1 = \left[\left(\frac{dT}{dr} \right)^2 + \left(\frac{Nu}{Pe} \right)^2 \right], \quad (17)$$

The entropy generation due to viscous dissipation is given by

$$Ns_2 = T_0 Br \left[\frac{u^2}{Da} + \mu_R \left(\frac{du}{dr} \right)^2 \right] \quad (18)$$

and entropy generation due to magnetic field is given by,

$$Ns_3 = T_0 Br M^2 u^2. \quad (19)$$

The Bejan number Be is given by

$$Be = \frac{Ns_1}{Ns} \quad (20)$$

3. APPROXIMATE ANALYTICAL EXPRESSIONS OF THE NON-LINEAR BOUNDARY VALUE PROBLEM USING THE HOMOTOPY ANALYSIS METHOD (HAM)

Using the HAM, the initial and first approximations of velocity profile are as follows:

$$u_0 = \frac{-r^2}{2\mu_1} + \frac{1+2\alpha}{2\mu_1} \quad (21)$$

$$u_1 = C_1 - \left[\frac{\eta^2}{2M\mu_1} + \frac{M^2}{2\mu_1^2} \right] \frac{r^4}{12} + \left[\frac{1}{\mu_1} + \frac{(1+2\alpha)\eta^2}{2M\mu_1} + \frac{M^2(1+2\alpha)}{2\mu_1^2} \right] \frac{r^2}{2} \quad (22)$$

where

$$C_1 = \frac{1}{12} \left[\frac{\eta^2}{2M\mu_1} + \frac{M^2}{2\mu_1^2} \right] (1+4\alpha) - \frac{1}{2} \left[\frac{1}{\mu_1} + \frac{(1+2\alpha)\eta^2}{2M\mu_1} + \frac{M^2(1+2\alpha)}{2\mu_1^2} \right] (1+2\alpha) \quad (23)$$

The approximate analytical expression of the velocity profile is as follows:

$$u = u_0 - hu_1 = \frac{-r^2}{2\mu_1} + \frac{1+2\alpha}{2\mu_1} - h \left(C_1 - \left[\frac{\eta^2}{2M\mu_1} + \frac{M^2}{2\mu_1^2} \right] \frac{r^4}{12} + \left[\frac{1}{\mu_1} + \frac{(1+2\alpha)\eta^2}{2M\mu_1} + \frac{M^2(1+2\alpha)}{2\mu_1^2} \right] \frac{r^2}{2} \right) \quad (24)$$

where C_1 is as defined in an eqn.(23).

Using HAM, the initial and first approximations of the temperature profiles are as follows:

$$T_0 = \frac{-\beta r^2}{2} + \beta^2 + \frac{\beta}{2} \quad (25)$$

$$T_1 = C_2 - \left[\frac{(\eta^2 + M^2)BrL}{\mu_1^2} \right] \frac{r^6}{120} + \left[\frac{NuL}{2\mu_1} + \frac{(1+2\alpha)(\eta^2 + M^2)BrL}{2\mu_1^2} \right] \frac{r^4}{12} + \left[\frac{Br\mu_r L}{\mu_1} \right] \frac{r^3}{6} \\ + \left[2\beta - \frac{(1+2\alpha)NuL}{2\mu_1} - \frac{(1+2\alpha)(\eta^2 + M^2)BrL}{4\mu_1^2} \right] \frac{r^2}{2} \quad (26)$$

where

$$C_2 = \frac{1}{120} \left[\frac{(\eta^2 + M^2)BrL}{\mu_1^2} \right] (1+6\beta) - \frac{1}{12} \left[\frac{NuL}{2\mu_1} + \frac{(1+2\alpha)(\eta^2 + M^2)BrL}{2\mu_1^2} \right] (1+4\beta) \\ - \frac{1}{6} \left[\frac{Br\mu_r L}{\mu_1} \right] (1+3\beta) - \frac{1}{2} \left[2\beta - \frac{(1+2\alpha)NuL}{2\mu_1} - \frac{(1+2\alpha)(\eta^2 + M^2)BrL}{4\mu_1^2} \right] (1+2\beta) \quad (27)$$

The approximate analytical expressions of the temperature profile are as follows:

$$T = T_0 - hT_1$$

$$= \frac{-\beta r^2}{2} + \beta^2 + \frac{\beta}{2} - h \left(C_2 - \left[\frac{(\eta^2 + M^2)BrL}{\mu_1^2} \right] \frac{r^6}{120} + \left[\frac{NuL}{2\mu_1} + \frac{(1+2\alpha)(\eta^2 + M^2)BrL}{2\mu_1^2} \right] \frac{r^4}{12} + \left[\frac{Br\mu_r L}{\mu_1} \right] \frac{r^3}{6} + \left[2\beta - \frac{(1+2\alpha)NuL}{2\mu_1} - \frac{(1+2\alpha)(\eta^2 + M^2)BrL}{4\mu_1^2} \right] \frac{r^2}{2} \right) \quad (28)$$

where C_2 is defined as in eqn.(27).

The approximate analytical expression of the nusselt number is as follows:

$$\begin{aligned}
 Nu = & \left[\frac{1+2\alpha}{2\mu_1} + C_1 \right] \left[\frac{\beta^2}{2} + \frac{\beta}{4} + \frac{h(M^2 + \eta^2)BrL(1+6\beta)}{240\mu_1^2} + \frac{h(1+2\alpha)(\eta^2 + M^2)BrL}{48\mu_1^2} \right. \\
 & + \frac{h\beta(1+2\beta)}{2} + \frac{hBr\mu_R L(1+3\beta)}{12\mu_1} - \frac{h(1+2\alpha)^2(\eta^2 + M^2)BrL(1+2\beta)}{16\mu_1^2} \\
 & - \frac{h\beta}{8} - \frac{\beta}{16} - \frac{hBr\mu_R L}{30\mu_1} + \frac{h(\eta^2 + M^2)BrL}{840\mu_1^2} + \frac{h(1+2\alpha)^2(\eta^2 + M^2)BrL}{64\mu_1^2} \\
 & \left. - \frac{h(1+2\alpha)(\eta^2 + M^2)BrL}{144\mu_1^2} \right] \\
 & + \left[\frac{-h}{\mu_1} - \frac{h(1+2\alpha)\eta^2}{2M\mu_1} \right] \left[\frac{\beta^2}{8} + \frac{\beta}{16} - \frac{h(M^2 + \eta^2)BrL(1+6\beta)}{960\mu_1^2} + \frac{h\beta(1+2\beta)}{8} \right. \\
 & - \frac{hBr\mu_R L}{42\mu_1} + \frac{hBr\mu_R L(1+3\beta)}{48\mu_1} + \frac{h(\eta^2 + M^2)BrL}{1200\mu_1^2} \\
 & + \frac{h(1+2\alpha)(\eta^2 + M^2)BrL(1+4\beta)}{192\mu_1^2} \\
 & \left. - \frac{h(1+2\alpha)^2(\eta^2 + M^2)BrL(1+2\beta)}{64\mu_1^2} \right. \\
 & \left. - \frac{h(1+2\alpha)(\eta^2 + M^2)BrL}{384\mu_1^2} \right] \\
 & + \left[\frac{h\eta^2}{24M\mu_1} + \frac{hM^2}{24\mu_1^2} \right] \left[\frac{\beta^2}{6} + \frac{\beta}{12} - \frac{h(M^2 + \eta^2)BrL(1+6\beta)}{720\mu_1^2} + \frac{h(1+2\alpha)(\eta^2 + M^2)BrL(1+4\beta)}{144\mu_1^2} \right. \\
 & + \frac{h\beta(1+2\beta)}{6} + \frac{hBr\mu_R L(1+3\beta)}{36\mu_1} - \frac{h(1+2\alpha)^2(\eta^2 + M^2)BrL(1+2\beta)}{48\mu_1^2} \\
 & - \frac{h\beta}{8} - \frac{\beta}{16} - \frac{hBr\mu_R L}{54\mu_1} + \frac{h(\eta^2 + M^2)BrL}{1440\mu_1^2} - \frac{h(1+2\alpha)^2(\eta^2 + M^2)BrL}{32\mu_1^2} \\
 & \left. - \frac{h(1+2\alpha)(\eta^2 + M^2)BrL}{240\mu_1^2} \right] \\
 & \left[\frac{1+2\alpha}{2\mu_1} + C_1 \right] \left[\frac{hL(1+4\beta)}{48\mu_1} - \frac{h(1+2\alpha)L(1+2\beta)}{8\mu_1} + \frac{h(1+2\alpha)L}{16\mu_1} - \frac{hL}{144\mu_1} \right] + \left[\frac{-h}{\mu_1} - \frac{h(1+2\alpha)\eta^2}{2M\mu_1} \right. \\
 & \left. - \frac{hM^2(1+2\alpha)}{2\mu_1^2} - \frac{1}{\mu_1} \right] \\
 & \left[\frac{hL(1+4\beta)}{192\mu_1} - \frac{h(1+2\alpha)L(1+2\beta)}{32\mu_1} + \frac{h(1+2\alpha)L}{24\mu_1} - \frac{hL}{384\mu_1} \right] + \left[\frac{h\eta^2}{24M\mu_1} + \frac{hM^2}{24\mu_1^2} \right] \left[\frac{hL(1+4\beta)}{144\mu_1} \right. \\
 & \left. - \frac{h(1+2\alpha)L(1+2\beta)}{24\mu_1} \right. \\
 & \left. + \frac{h(1+2\alpha)L}{32\mu_1} - \frac{hL}{24\mu_1} \right]
 \end{aligned}
 \tag{29}$$

where C_1 is as defined in (3).

The approximate analytical expression of the entropy generation rate is given as follows:

$$\begin{aligned}
 N_s = & \left[-\beta r - h \left(- \left[\frac{(\eta^2 + M^2)BrL}{\mu_1^2} \right] \frac{r^5}{20} + \left[\frac{NuL}{2\mu_1} + \frac{(1+2\alpha)(\eta^2 + M^2)BrL}{2\mu_1^2} \right] \frac{r^3}{3} \right. \right. \\
 & \left. \left. + \left[\frac{Br\mu_r L}{\mu_1} \right] \frac{r^2}{2} + \left[2\beta - \frac{(1+2\alpha)NuL}{2\mu_1} - \frac{(1+2\alpha)(\eta^2 + M^2)BrL}{4\mu_1^2} \right] r \right) \right]^2 + \left[\frac{Nu}{Pe} \right]^2 \\
 & + \left[\frac{-\beta r^2}{2} + \beta^2 + \frac{\beta}{2} - h \left(C_2 - \left[\frac{(\eta^2 + M^2)BrL}{\mu_1^2} \right] \frac{r^6}{120} \right. \right. \\
 & \left. \left. + \left[\frac{NuL}{2\mu_1} + \frac{(1+2\alpha)(\eta^2 + M^2)BrL}{2\mu_1^2} \right] \frac{r^4}{12} + \left[\frac{Br\mu_r L}{\mu_1} \right] \frac{r^3}{6} \right. \right. \\
 & \left. \left. + \left[2\beta - \frac{(1+2\alpha)NuL}{2\mu_1} - \frac{(1+2\alpha)(\eta^2 + M^2)BrL}{4\mu_1^2} \right] \frac{r^2}{2} \right) \right]^2 Br \\
 & + \left[\frac{\left(\frac{-r^2}{2\mu_1} + \frac{1+2\alpha}{2\mu_1} - h \left(C_1 - \left[\frac{\eta^2}{2M\mu_1} + \frac{M^2}{2\mu_1^2} \right] \frac{r^4}{12} + \left[\frac{1}{\mu_1} + \frac{(1+2\alpha)\eta^2}{2M\mu_1} + \frac{M^2(1+2\alpha)}{2\mu_1^2} \right] \frac{r^2}{2} \right) \right)^2}{Da} + \right. \\
 & \left. \mu_R \left(\frac{-r}{\mu_1} - h \left(- \left[\frac{\eta^2}{2M\mu_1} + \frac{M^2}{2\mu_1^2} \right] \frac{r^3}{3} + \left[\frac{1}{\mu_1} + \frac{(1+2\alpha)\eta^2}{2M\mu_1} + \frac{M^2(1+2\alpha)}{2\mu_1^2} \right] r \right) \right)^2 \right] \\
 & + \left[\frac{-\beta r^2}{2} + \beta^2 + \frac{\beta}{2} - h \left(C_2 - \left[\frac{(\eta^2 + M^2)BrL}{\mu_1^2} \right] \frac{r^6}{120} + \left[\frac{NuL}{2\mu_1} + \frac{(1+2\alpha)(\eta^2 + M^2)BrL}{2\mu_1^2} \right] \frac{r^4}{12} \right. \right. \\
 & \left. \left. + \left[\frac{Br\mu_r L}{\mu_1} \right] \frac{r^3}{6} + \left[2\beta - \frac{(1+2\alpha)NuL}{2\mu_1} - \frac{(1+2\alpha)(\eta^2 + M^2)BrL}{4\mu_1^2} \right] \frac{r^2}{2} \right) \right]^2 \\
 & + \left[BrM^2 \left(\frac{-r^2}{2\mu_1} + \frac{1+2\alpha}{2\mu_1} - h \left(C_1 - \left[\frac{\eta^2}{2M\mu_1} + \frac{M^2}{2\mu_1^2} \right] \frac{r^4}{12} + \left[\frac{1}{\mu_1} + \frac{(1+2\alpha)\eta^2}{2M\mu_1} + \frac{M^2(1+2\alpha)}{2\mu_1^2} \right] \frac{r^2}{2} \right) \right)^2 \right]^2
 \end{aligned}
 \tag{30}$$

The approximate analytical expressions of the Bejan number is as follows:

$$\begin{aligned}
 Be = & \frac{\left[-\beta r - h \left(- \left[\frac{(\eta^2 + M^2)BrL}{\mu_1^2} \right] \frac{r^5}{20} + \left[\frac{NuL}{2\mu_1} + \frac{(1+2\alpha)(\eta^2 + M^2)BrL}{2\mu_1^2} \right] \frac{r^3}{3} \right. \right. \\
 & \left. \left. + \left[\frac{Br\mu_r L}{\mu_1} \right] \frac{r^2}{2} + \left[2\beta - \frac{(1+2\alpha)NuL}{2\mu_1} - \frac{(1+2\alpha)(\eta^2 + M^2)BrL}{4\mu_1^2} \right] r \right) \right]^2 + \left[\frac{Nu}{Pe} \right]^2}{\left[-\beta r - h \left(- \left[\frac{(\eta^2 + M^2)BrL}{\mu_1^2} \right] \frac{r^5}{20} + \left[\frac{NuL}{2\mu_1} + \frac{(1+2\alpha)(\eta^2 + M^2)BrL}{2\mu_1^2} \right] \frac{r^3}{3} \right. \right. \\
 & \left. \left. + \left[\frac{Br\mu_r L}{\mu_1} \right] \frac{r^2}{2} + \left[2\beta - \frac{(1+2\alpha)NuL}{2\mu_1} - \frac{(1+2\alpha)(\eta^2 + M^2)BrL}{4\mu_1^2} \right] r \right) \right]^2 + \left[\frac{Nu}{Pe} \right]^2} \\
 & + \left[\frac{-\beta r^2}{2} + \beta^2 + \frac{\beta}{2} - h \left(C_2 - \left[\frac{(\eta^2 + M^2)BrL}{\mu_1^2} \right] \frac{r^6}{120} + \left[\frac{NuL}{2\mu_1} + \frac{(1+2\alpha)(\eta^2 + M^2)BrL}{2\mu_1^2} \right] \frac{r^4}{12} \right. \right. \\
 & \left. \left. + \left[\frac{Br\mu_r L}{\mu_1} \right] \frac{r^3}{6} + \left[2\beta - \frac{(1+2\alpha)NuL}{2\mu_1} - \frac{(1+2\alpha)(\eta^2 + M^2)BrL}{4\mu_1^2} \right] \frac{r^2}{2} \right) \right]^2 Br \\
 & \left[\frac{\left(\frac{-r^2}{2\mu_1} + \frac{1+2\alpha}{2\mu_1} - h \left(C_1 - \left[\frac{\eta^2}{2M\mu_1} + \frac{M^2}{2\mu_1^2} \right] \frac{r^4}{12} + \left[\frac{1}{\mu_1} + \frac{(1+2\alpha)\eta^2}{2M\mu_1} + \frac{M^2(1+2\alpha)}{2\mu_1^2} \right] \frac{r^2}{2} \right) \right)^2}{Da} + \right. \\
 & \left. \mu_R \left(\frac{-r}{\mu_1} - h \left(- \left[\frac{\eta^2}{2M\mu_1} + \frac{M^2}{2\mu_1^2} \right] \frac{r^3}{3} + \left[\frac{1}{\mu_1} + \frac{(1+2\alpha)\eta^2}{2M\mu_1} + \frac{M^2(1+2\alpha)}{2\mu_1^2} \right] r \right) \right)^2 \right] \\
 & + \left[\frac{-\beta r^2}{2} + \beta^2 + \frac{\beta}{2} - h \left(C_2 - \left[\frac{(\eta^2 + M^2)BrL}{\mu_1^2} \right] \frac{r^6}{120} + \left[\frac{NuL}{2\mu_1} + \frac{(1+2\alpha)(\eta^2 + M^2)BrL}{2\mu_1^2} \right] \frac{r^4}{12} \right. \right. \\
 & \left. \left. + \left[\frac{Br\mu_r L}{\mu_1} \right] \frac{r^3}{6} + \left[2\beta - \frac{(1+2\alpha)NuL}{2\mu_1} - \frac{(1+2\alpha)(\eta^2 + M^2)BrL}{4\mu_1^2} \right] \frac{r^2}{2} \right) \right]^2 \\
 & BrM^2 \left[\frac{-r^2}{2\mu_1} + \frac{1+2\alpha}{2\mu_1} - h \left(C_1 - \left[\frac{\eta^2}{2M\mu_1} + \frac{M^2}{2\mu_1^2} \right] \frac{r^4}{12} + \left[\frac{1}{\mu_1} + \frac{(1+2\alpha)\eta^2}{2M\mu_1} + \frac{M^2(1+2\alpha)}{2\mu_1^2} \right] \frac{r^2}{2} \right) \right]^2
 \end{aligned} \tag{31}$$

4. RESULTS AND DISCUSSION

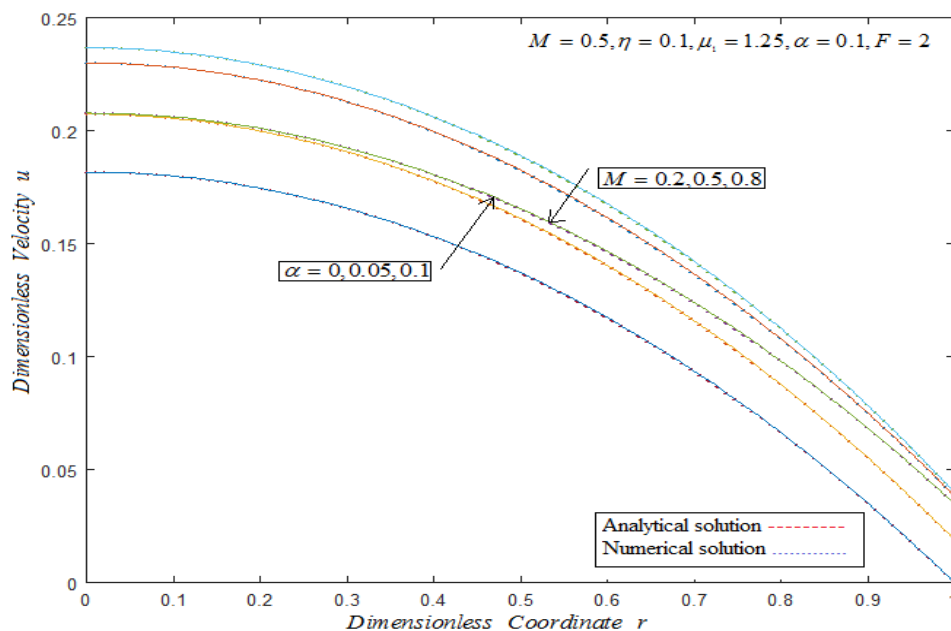


Fig:2 Dimensionless coordinate r versus dimensionless velocity profile u . The curves are plotted using the eqn.(24) for fixed η, μ_1, F and varying M and α .

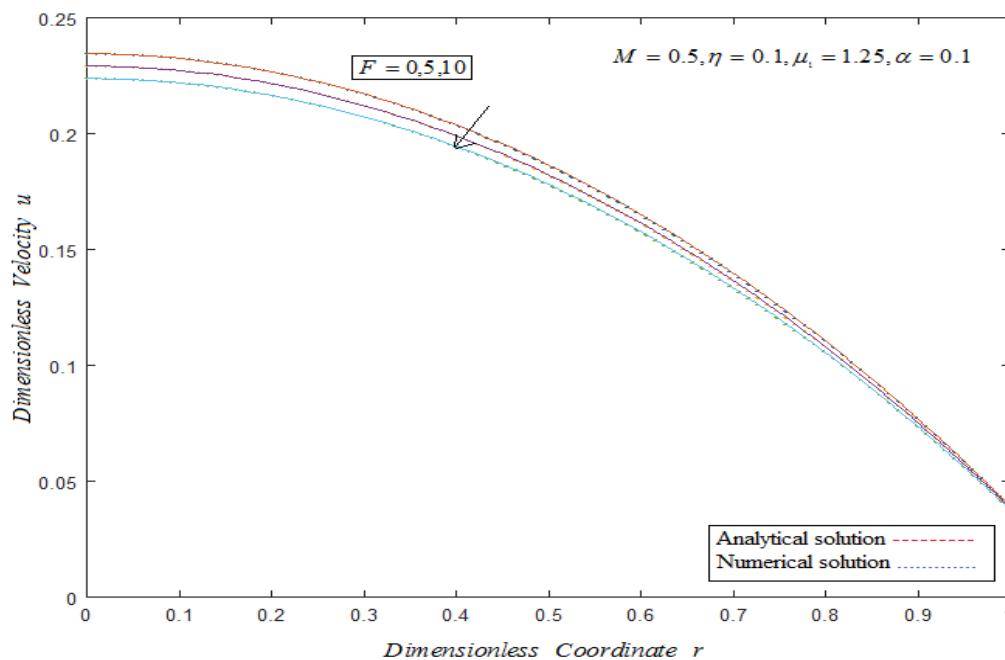


Fig:3 Dimensionless coordinate r versus dimensionless velocity profile u . The curves are plotted using the eqn.(24) for fixed η, μ_1, M, α and varying F .

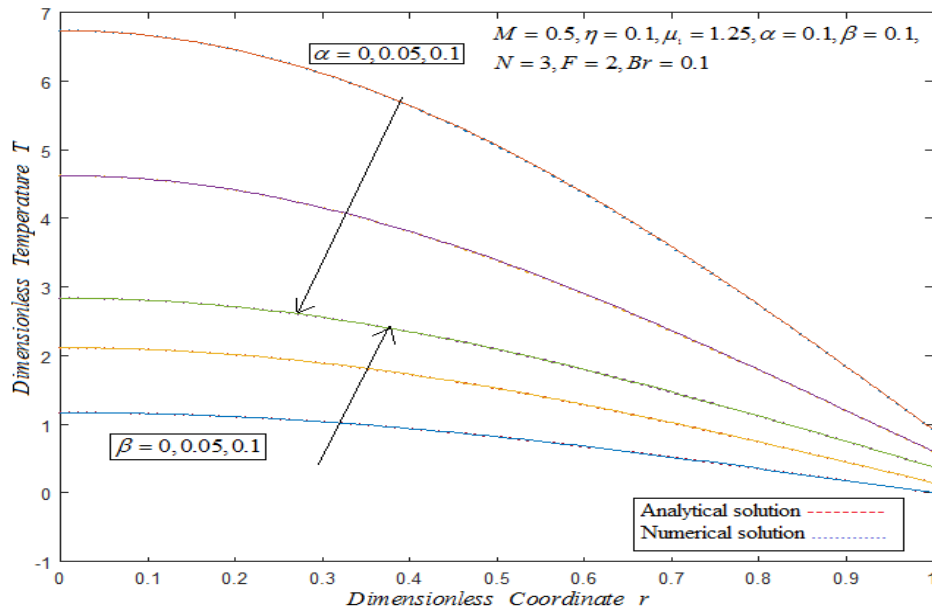


Fig:4 Dimensionless coordinate r versus dimensionless temperature profile T . The curves are plotted using the eqn.(28) for fixed M, η, μ_1, Br, F, N and varying α and β .

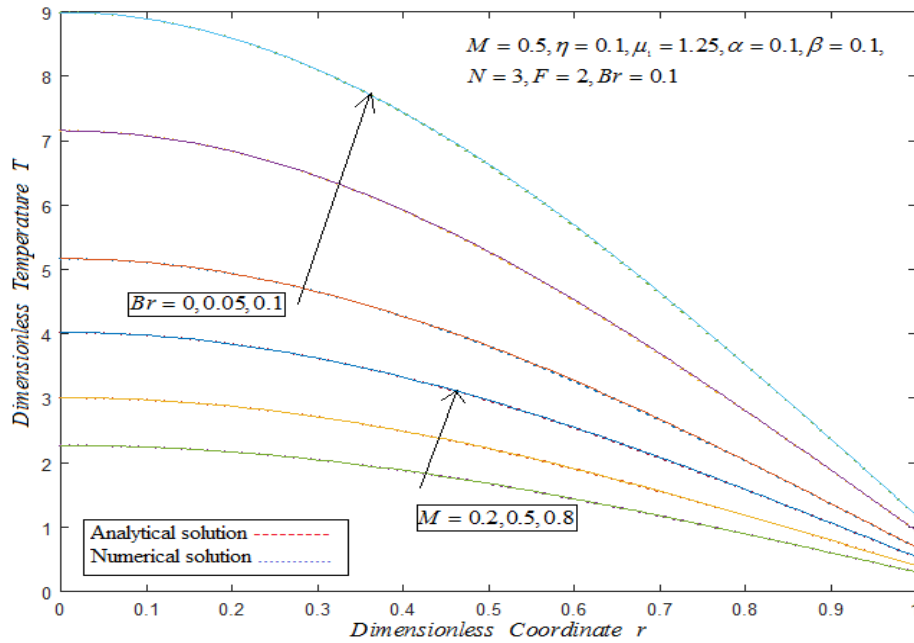


Fig:5 Dimensionless coordinate r versus dimensionless temperature profile T . The curves are plotted using the eqn. (28) for fixed $\eta, \mu_1, \alpha, \beta, F, N$ and varying M and Br .

ENTROPY ANALYSIS IN MHD FORCED CONVECTIVE FLOW

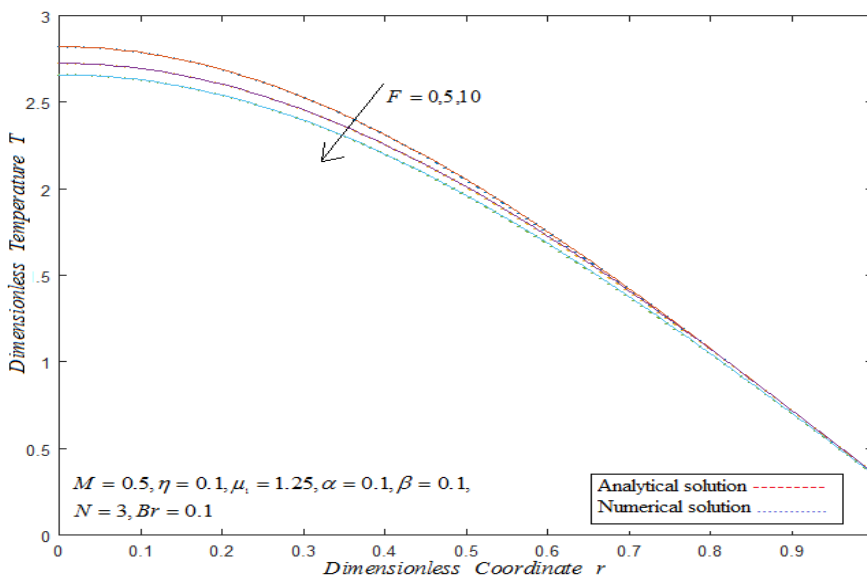


Fig:6 Dimensionless coordinate r versus dimensionless temperature profile T . The curves are plotted using the eqn.(28) for fixed $M, \eta, \mu_1, \alpha, \beta, Br, N$ and varying F .

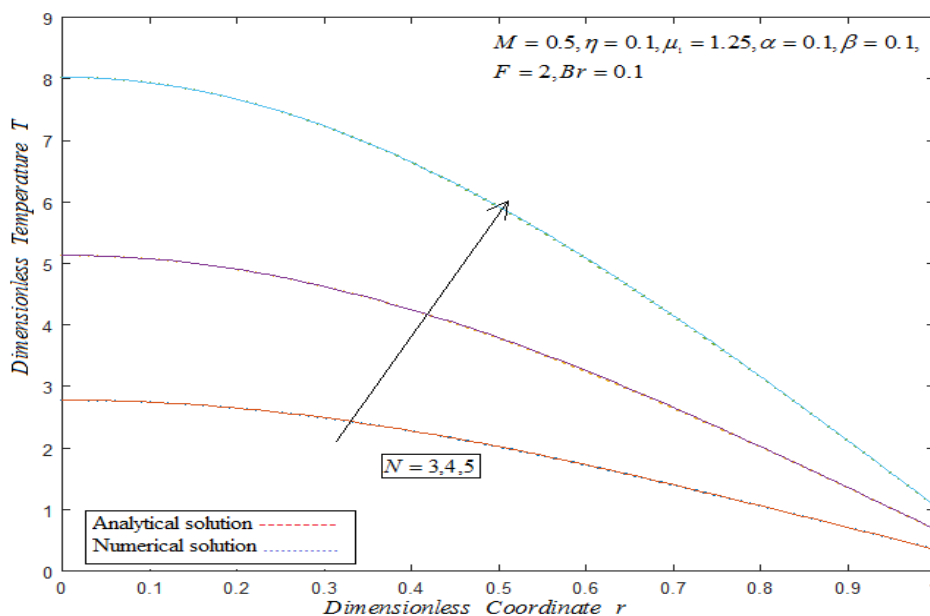


Fig:7 Dimensionless coordinate r versus dimensionless temperature profile T . The curves are plotted using the eqn.(28) for fixed $M, \eta, \mu_1, \alpha, \beta, Br, F$ and varying N .

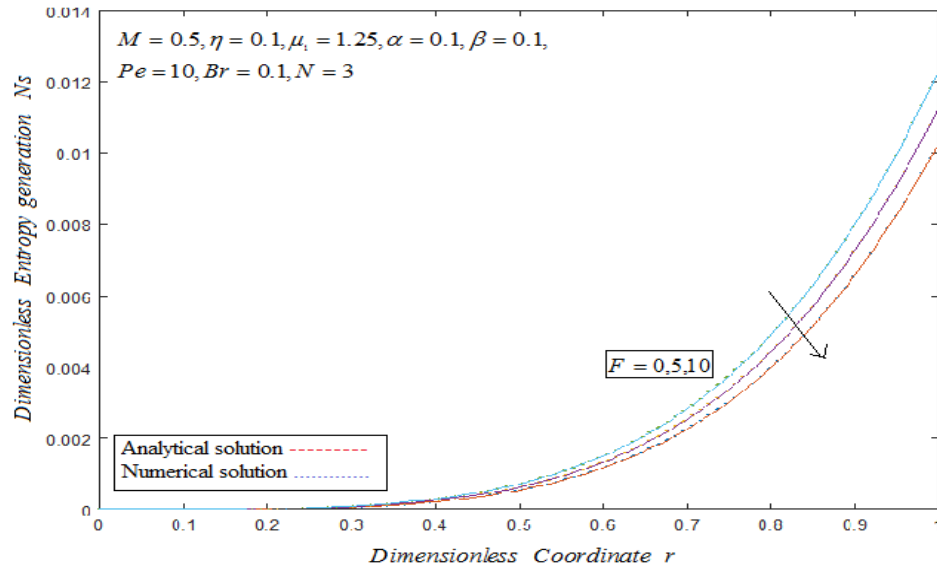


Fig:8 Dimensionless coordinate r versus dimensionless entropy generation N_s . The curves are plotted using the eqn.(30) for fixed $M, \eta, \mu_1, \alpha, \beta, Br, Pe, N$ and varying F .

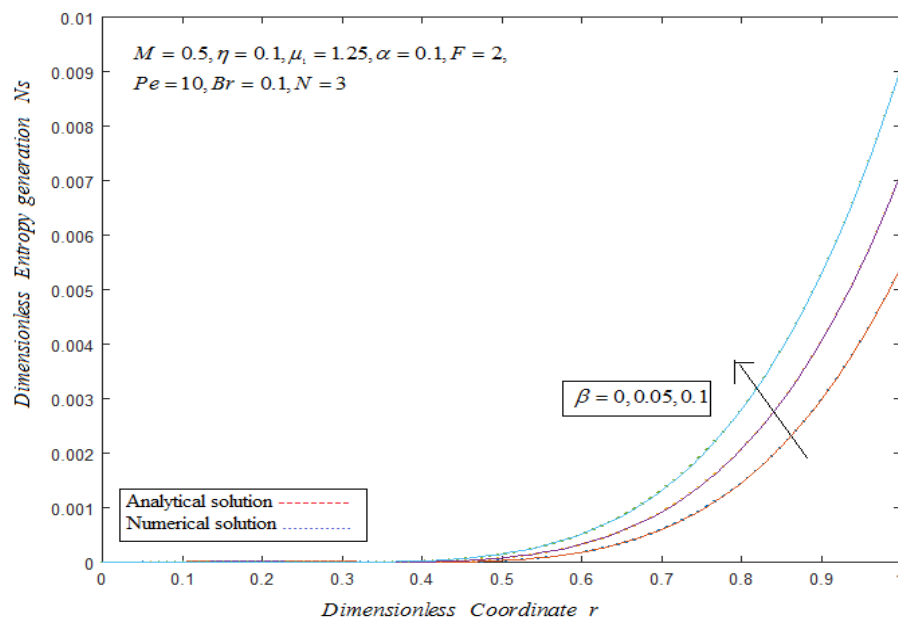


Fig:9 Dimensionless coordinate r versus dimensionless entropy generation N_s . The curves are plotted using the eqn.(30) for fixed $M, \eta, \mu_1, \alpha, Br, Pe, F, N$ and varying β .

ENTROPY ANALYSIS IN MHD FORCED CONVECTIVE FLOW

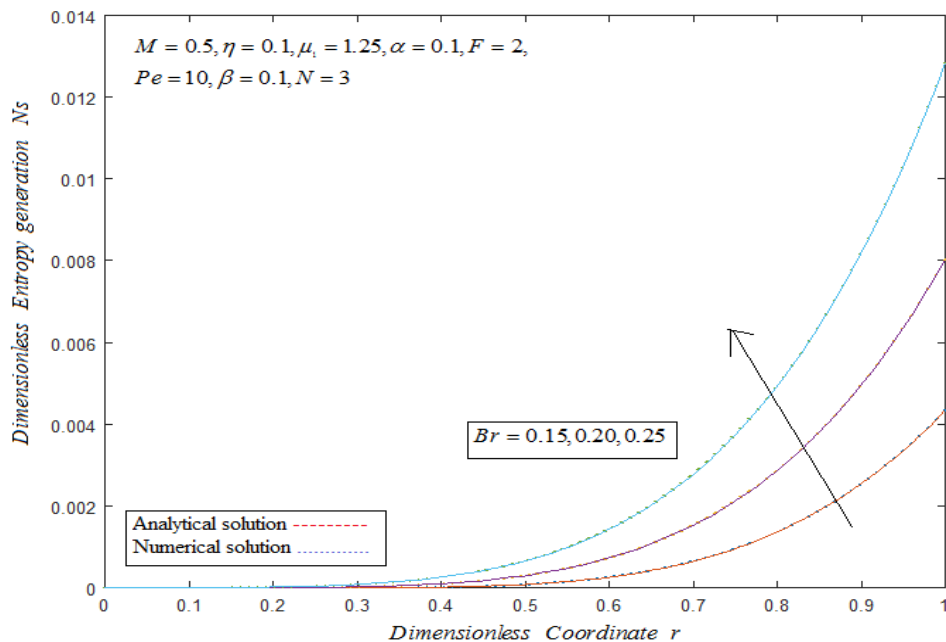


Fig:10 Dimensionless coordinate r versus dimensionless entropy generation N_s . The curves are plotted using the eqn.(30) for fixed $M, \eta, \mu_1, \alpha, \beta, Pe, F, N$ and varying Br .

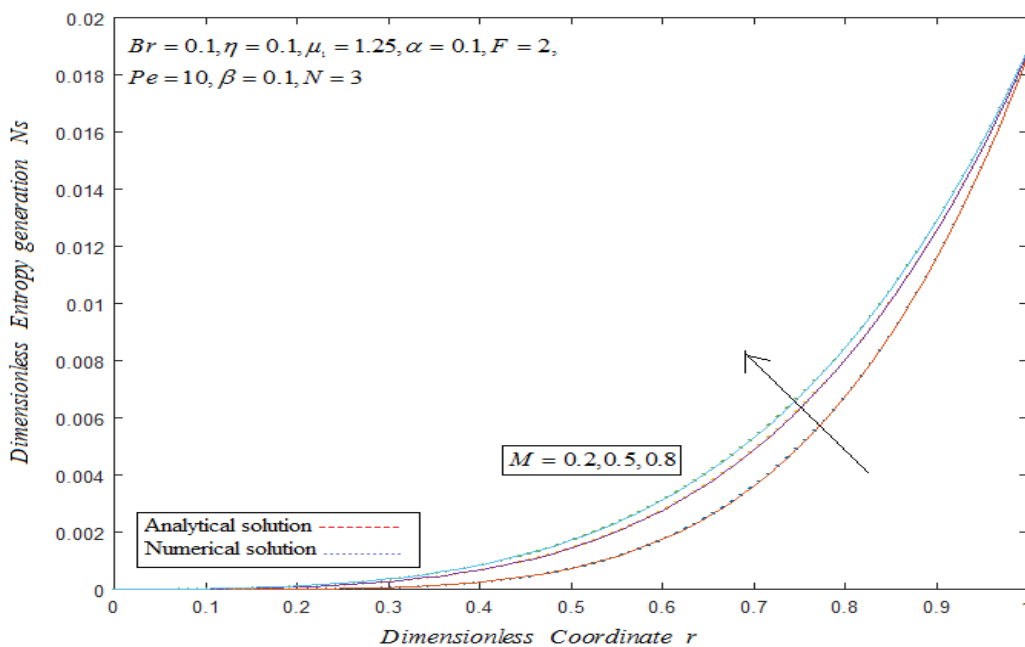


Fig:11 Dimensionless coordinate r versus dimensionless entropy generation N_s . The curves are plotted using the eqn.(30) for fixed $\eta, \mu_1, \alpha, \beta, Br, Pe, F, N$ and varying M .

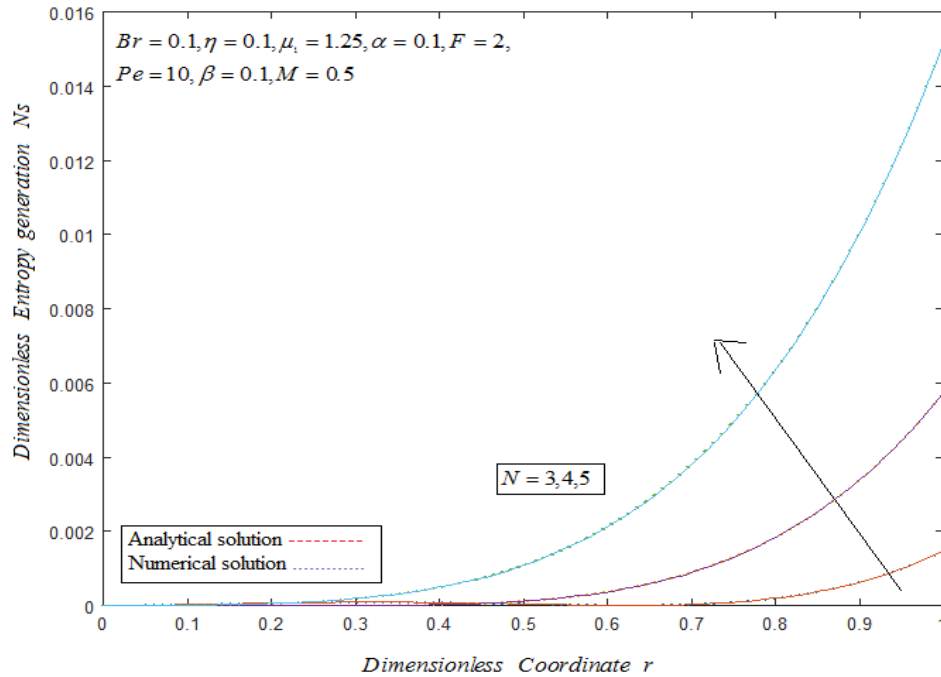


Fig:12 Dimensionless coordinate r versus dimensionless entropy generation N_s . The curves are plotted using the eqn.(30) for fixed $M, \eta, \mu_1, \alpha, \beta, Br, Pe, F$ and varying N

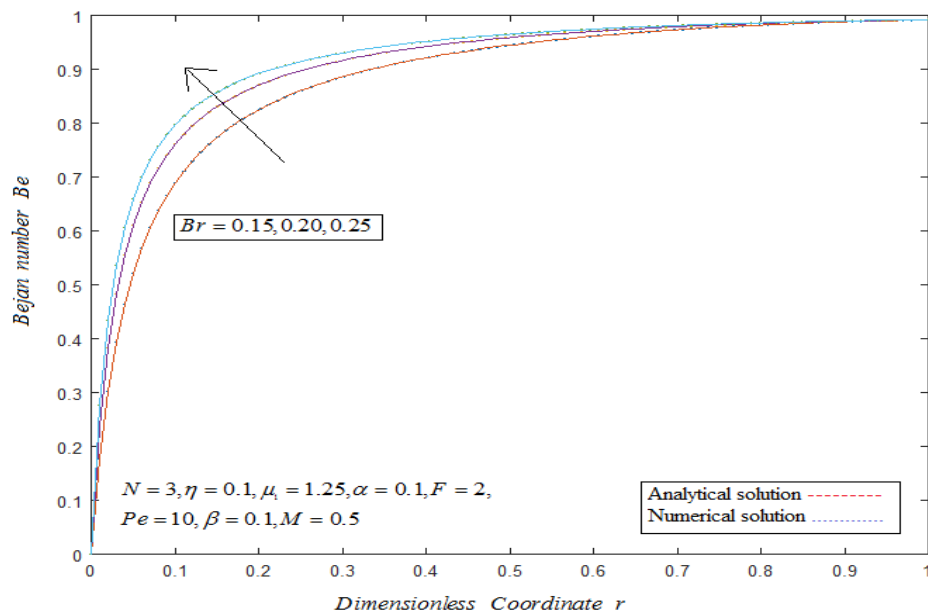


Fig:13 Dimensionless coordinate r versus Bejan number Be . The curves are plotted using (31) for fixed $M, \eta, \mu_1, \alpha, \beta, Pe, F, N$ and varying Br .

ENTROPY ANALYSIS IN MHD FORCED CONVECTIVE FLOW

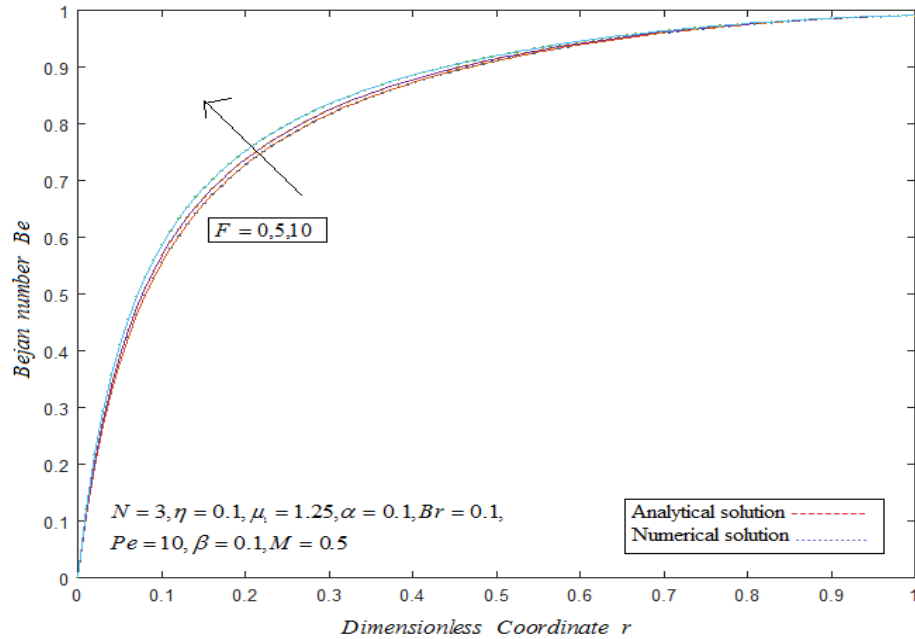


Fig:14 Dimensionless coordinate r versus Bejan number Be . The curves are plotted using the eqn.(31) for fixed $M, \eta, \mu_1, \alpha, \beta, Br, Pe, N$ and varying F .

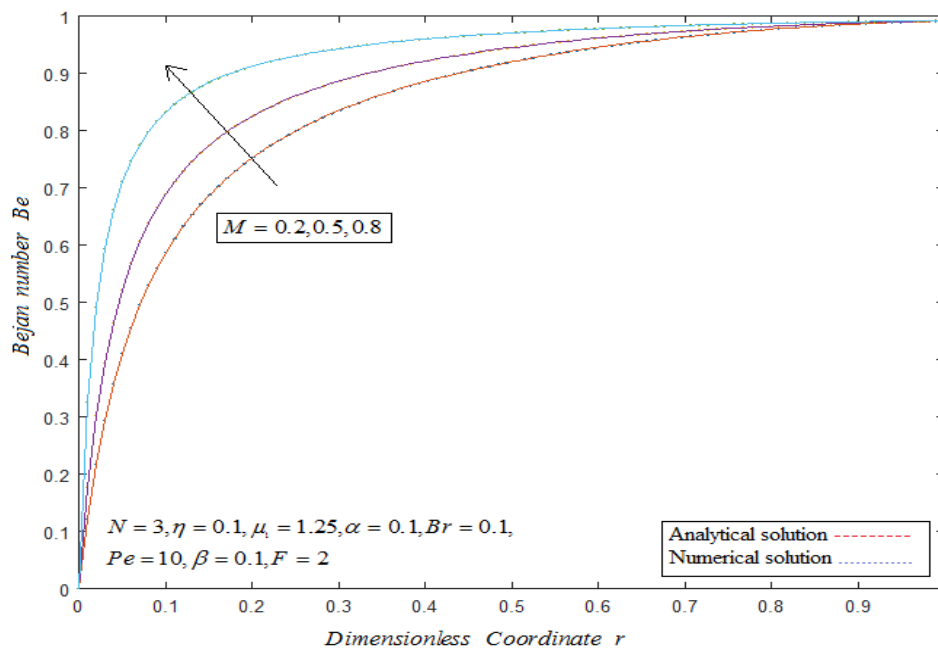


Fig:15 Dimensionless coordinate r versus Bejan number Be . The curves are plotted using the eqn.(31) for fixed $M, \eta, \mu_1, \alpha, \beta, Br, Pe, F, N$ and varying M .

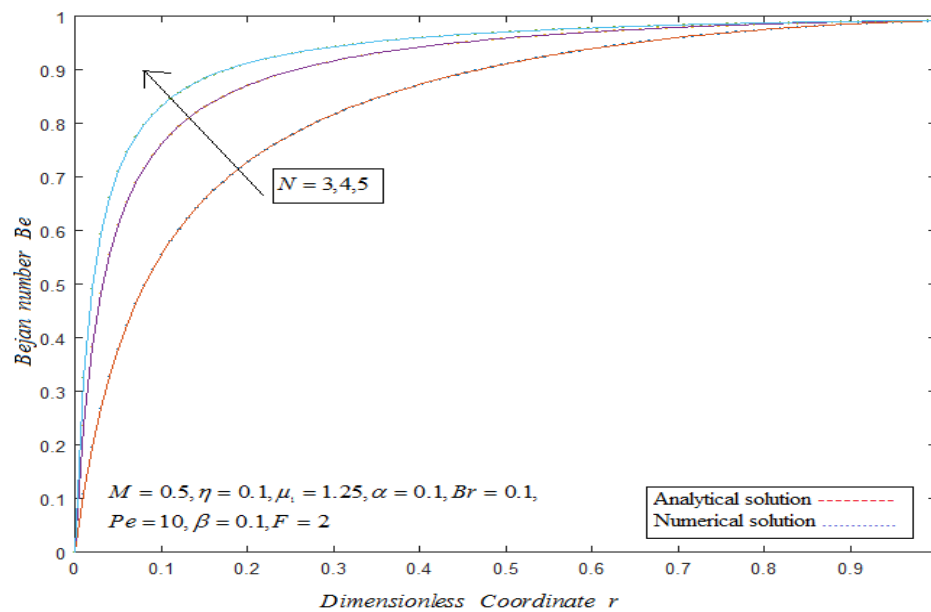


Fig:16. Dimensionless coordinate r versus Bejan number Be . The curves are plotted using the eqn.(31) for fixed $M, \eta, \mu_1, \alpha, \beta, Br, Pe, F$ and varying N .

Figures 2 and 3 denote the dimensionless velocity profile with respect to the dimensionless coordinate r . From Fig.2, we find that due to the increase in the intensity of the magnetic field M , the velocity decreases. Also we observe that due to the increase in the slip parameter α , the velocity increases. From Fig.3, we observe that the velocity decreases as the forchheimer number F increases. From the above two Figs., we observe that the velocity is high at the centre of the circular tube.

Figures 4 to 7 represents that the dimensionless temperature profile with respect to the dimensionless coordinate r . From Fig.4, it is observed that the temperature decreases as the slip parameter α increases and the temperature increases as the temperature slip parameter β increases. From Fig.5, we observe that the temperature increases as the Brinkmann number increases. Also the temperature increases with the magnetic field M . From Fig.6, we observe that the temperature decreases with the forchheimer number. From Fig.7, it follows that the temperature increases with the radiation parameter N . From these four Figs., we observe that the temperature is high at the centre of the circular tube.

The Figures 8 to 12 indicate that the dimensionless entropy generation N_s with respect to the dimensionless coordinate r . From Fig.8, it is observed that the entropy generation becomes lower as the forchheimer number F increases. From Fig.9, we find that the entropy generation increases with the temperature slip parameter β . From Fig.10, we observe that the entropy generation becomes higher as the Brinkmann number increases and from Fig.11, we observe that the entropy generation becomes larger with Hartman number M . From Fig.12, we observe that the entropy generation increases with the radiation parameter N .

Figures 13 to 16 depict the Bejan number Be with respect to the dimensionless coordinate r . From these Figs., we observe that the Bejan number becomes higher with the radiation parameter N , the Brinkmann number Br , the Forchheimer number F and Hartman number M . Moreover we see that the Bejan number attains its maximum value.

5. CONCLUSION

In this paper, we investigated the flow of a viscous incompressible fluid within a circular channel concentrated with low density gas in the midst of a transverse magnetic field, thermal radiation and uniform heat flux on the walls. The velocity and heat equations were solved analytically using the Homotopy Analysis Method (HAM) and using them the entropy generation, the Bejan number and the Nusselt number were determined. The results were discussed graphically and the findings were conformed with the previous work.

APPENDIX: A

Approximate analytical expressions of the non-linear differential eqns.(8), (9), (13) and (14) using the Homotopy analysis method [12 – 19]

In this Appendix, how we derive the eqns. (24) and (27) using the Homotopy analysis method.

The differential equations are

$$\frac{d^2u}{dr^2} + \frac{1}{r} \frac{du}{dr} - \frac{\eta^2}{M} u - \frac{M^2}{\mu_1} u - \frac{F\eta}{\mu_1} + \frac{1}{\mu_1} = 0 \quad (\text{A.1})$$

$$\frac{d^2T}{dr^2} + \frac{1}{r} \frac{dT}{dr} + (Nu)uL + \eta^2 Bru^2L + Br\mu_R L \left(\frac{du}{dr} \right)^2 + M^2 Bru^2L = 0 \quad (\text{A.2})$$

With initial conditions

$$\begin{aligned} \frac{du}{dr} = 0, \frac{dT}{dr} = 0 \text{ at } r = 0 \\ u = -\alpha \frac{du}{dr}, T = -\beta \frac{dT}{dr} \text{ at } r = 1 \end{aligned} \quad (\text{A.3})$$

We construct the Homotopy for the eqns. (A.1) and (A.2) are as follows:

$$(1-p) \left[\frac{d^2u}{dr^2} + \frac{1}{\mu_1} \right] + p \left[\frac{d^2u}{dr^2} + \frac{1}{r} \frac{du}{dr} - \frac{\eta^2}{M} u - \frac{M^2}{\mu_1} u - \frac{F\eta}{\mu_1} + \frac{1}{\mu_1} \right] = 0 \quad (\text{A.4})$$

$$(1-p) \left[\frac{d^2T}{dr^2} + \beta \right] + p \left[\frac{d^2T}{dr^2} + \frac{1}{r} \frac{dT}{dr} + (Nu)uL + \eta^2 Bru^2L + Br\mu_R L \left(\frac{du}{dr} \right)^2 + M^2 Bru^2L - \beta \right] = 0 \quad (\text{A.5})$$

Let the approximate analytical solution of the eqns. (A.1) and (A.2)

$$u = u_0 + pu_1 + p^2u_2 + \dots \quad (\text{A.6})$$

$$T = T_0 + pT_1 + p^2T_2 + \dots \quad (\text{A.7})$$

Substituting the eqns.(A.6), (A.7) into the eqns. (A.4), (A.5) and comparing the coefficients of the powers of p we get the following eqns.

$$p^0: \frac{d^2u_0}{dr^2} + \frac{1}{\mu_1} = 0 \quad (\text{A.8})$$

$$p^1: \frac{d^2u_1}{dr^2} + \frac{1}{r} \frac{du_0}{dr} - \frac{\eta^2}{M} u_0 - \frac{M^2}{\mu_1} u_0 - \frac{F\eta}{\mu_1} = 0 \quad (\text{A.9})$$

$$p^0: \frac{d^2T_0}{dr^2} + \beta = 0 \quad (\text{A.10})$$

$$p^1: \frac{d^2T_1}{dr^2} + \frac{1}{r} \frac{dT_0}{dr} + (Nu)u_0L + \eta^2 Bru_0^2L + Br\mu_R L \left(\frac{du_0}{dr} \right)^2 + M^2 Bru_0^2L - 2\beta = 0 \quad (\text{A.11})$$

The initial approximations are as follows:

$$\frac{du_i}{dr} = 0, \frac{dT_i}{dr} = 0 \text{ at } r = 0, \quad i = 0,1,2,\dots \quad (\text{A.12})$$

$$u_i = -\alpha \frac{du_i}{dr}, T_i = -\beta \frac{dT_i}{dr} \text{ at } r = 1, i = 0, 1, 2, \dots \quad (\text{A.13})$$

Solving the eqns.(A.8) - (A.11) and using the initial approximations eqns. (A.12) and (A.13), we obtain the following results.

$$u_0 = \frac{-r^2}{2\mu_1} + \frac{1+2\alpha}{2\mu_1} \quad (\text{A.14})$$

$$u_1 = C_1 - \left[\frac{\eta^2}{2M\mu_1} + \frac{M^2}{2\mu_1^2} \right] \frac{r^4}{12} + \left[\frac{1}{\mu_1} + \frac{(1+2\alpha)\eta^2}{2M\mu_1} + \frac{M^2(1+2\alpha)}{2\mu_1^2} \right] \frac{r^2}{2} \quad (\text{A.15})$$

$$T_0 = \frac{-\beta r^2}{2} + \beta^2 + \frac{\beta}{2} \quad (\text{A.16})$$

$$T_1 = C_2 - \left[\frac{(\eta^2 + M^2)BrL}{\mu_1^2} \right] \frac{r^6}{120} + \left[\frac{NuL}{2\mu_1} + \frac{(1+2\alpha)(\eta^2 + M^2)BrL}{2\mu_1^2} \right] \frac{r^4}{12} + \left[\frac{Br\mu_r L}{\mu_1} \right] \frac{r^3}{6} \\ + \left[2\beta - \frac{(1+2\alpha)NuL}{2\mu_1} - \frac{(1+2\alpha)(\eta^2 + M^2)BrL}{4\mu_1^2} \right] \frac{r^2}{2} \quad (\text{A.17})$$

where

$$C_1 = \frac{1}{12} \left[\frac{\eta^2}{2M\mu_1} + \frac{M^2}{2\mu_1^2} \right] (1+4\alpha) - \frac{1}{2} \left[\frac{1}{\mu_1} + \frac{(1+2\alpha)\eta^2}{2M\mu_1} + \frac{M^2(1+2\alpha)}{2\mu_1^2} \right] (1+2\alpha) \quad (\text{A.18})$$

$$C_2 = \frac{1}{120} \left[\frac{(\eta^2 + M^2)BrL}{\mu_1^2} \right] (1+6\beta) - \frac{1}{12} \left[\frac{NuL}{2\mu_1} + \frac{(1+2\alpha)(\eta^2 + M^2)BrL}{2\mu_1^2} \right] (1+4\beta) \\ - \frac{1}{6} \left[\frac{Br\mu_r L}{\mu_1} \right] (1+3\beta) - \frac{1}{2} \left[2\beta - \frac{(1+2\alpha)NuL}{2\mu_1} - \frac{(1+2\alpha)(\eta^2 + M^2)BrL}{4\mu_1^2} \right] (1+2\beta) \quad (\text{A.19})$$

According to HAM we conclude that

$$u = \lim_{p \rightarrow 1} u(r) = u_0 - hu_1 \quad (\text{A.20})$$

$$T = \lim_{p \rightarrow 1} T(r) = T_0 - hT_1 \quad (\text{A.21})$$

Substituting the eqns.(A.14) and (A.15) into an eqn. (A.20) and substituting the eqns. (A.16) and (A.17) into an eqn.(A.21), we obtain the solutions in the text eqns. (24) and (28) respectively.

The obtained velocity profile and temperature profile are utilized to obtain the Nusselt number, Entropy generation and the Bejan number in the text eqns.(29), (30) and (31) respectively.

Appendix: B: Nomenclature

Symbols	Meaning
Br	Brinkmann number
Be	Bejan number
c_p	Specific heat
F	Forchheimer number
K	Thermal conductivity
\bar{K}	Permeability
M	Hartman number
N	Radiation parameter
N_s	Entropy generation coefficient
Nu	Nusselt number
P	Negative of applied pressure gradient in x direction
R	Radius of circular channel
T	Dimensionless temperature
T_w	Temperature at wall
A	Dimensionless velocity slip coefficient
B	Dimensionless temperature slip coefficient
μ	Dynamic viscosity
μ_1	Viscosity ratio

CONFLICT OF INTERESTS

The author(s) declare that there is no conflict of interests.

REFERENCES

- [1] P. Sharma, N. Kumar, T. Sharma, Entropy Analysis in MHD Forced Convective Flow through a Circular Channel Filled with Porous Medium in the Presence of Thermal Radiation, *Int. J. Heat Technol.* 34 (2016), 311–318.
- [2] A. Bejan., *Entropy Generation through Heat and Fluid Flow*, Wiley, New York, 1982.
- [3] A. Bejan, A study of entropy generation in fundamental convective heat transfer, *ASME J. Heat Transfer*, 101 (1979), 718 – 725.
- [4] A. Bejan, *Entropy Generation Minimization*, CRC Press, New York, 1996.
- [5] N. Ahmed. S. M. Das, Oscillatory MHD Mass Transfer Channel flow in a rotating System with hall current, *Int. J. Heat Technol.* 34 (2016), 115 -123.
- [6] B. Pakdemirli, S. Yilbas, Entropy generation in pipe due to non-Newtonian fluid flow constant viscosity case, *Sadhana*, 31 (2006), 21 – 29.
- [7] A. M. Bouchoucha, R. Bessaih, Natural convection and entropy generation of nanofluids in a square cavity, *Int. J. Heat Technol.* 33 (2015), 1 – 10.
- [8] P. Loganathan, C. Sivapoornapriya, Unsteady heat and mass transfer effect on an impulsively started infinite vertical plate in the in the presence of porous medium, *Int. J. Heat Technol.* 33 (2015), 69 – 74.
- [9] G. V. R. Reddy, N. B. Reddy, R. S. R. Gori, Radiation and chemical reaction effects on MHD flow along a moving vertical porous plate, *Int. J. Appl. Mech. Eng.* 21 (2016), 157 – 168.
- [10] O. Mahian, H. Oztop. L. Pop, S. Mahmud, S. Wongwises, Entropy Generation between two vertical cylinder in the presence of MHD flow subjected to constant wall temperature, *Int. Commun. Heat Mass Transfer*, 44 (2013), 87 – 92.
- [11] M. S. Tshela, O.D. Makinde, Analysis of entropy generation in a variable viscosity fluid flow between two concentric pipes with a convective cooling at the surface, *Int. J. Phys. Sci.* 6 (2011), 6053 – 6060.
- [12] V. Ananthaswamy, C. Sumathi, V. K. Shanthi., A mathematical study on MHD boundary layer flow of nanofluid and heat transfer over a porous exponentially stretching sheet, *Adv. Math., Sci. J.* 8 (2019), 109 – 130.
- [13] N. Kumar, S. Gupta, MHD forced convection and entropy generation in a circular channel occupied by hyper porous medium, *Heat Technol.* 29 (2011), 91 – 100.
- [14] S. J. Liao, The proposed Homotopy analysis technique for the solution of nonlinear Problems, Ph.D. Thesis,

Shanghai Jiao Tong University. 1992.

- [15] S.J. Liao, An approximate solution technique which does not depend upon small parameters: a special example, *Int. J. Non-Linear Mech.* 30 (1995), 371-380.
- [16] S.J. Liao, *Beyond Perturbation: Introduction to the Homotopy Analysis Method*. Chapman and Hall/CRC, Boca Raton, FL, 2003.
- [17] S.J. Liao, On the homotopy analysis method for nonlinear problems, *Applied Mathematics and Computation*. 147 (2004), 499–513.
- [18] S.J. Liao, An optimal homotopy-analysis approach for strongly nonlinear differential equations, *Commun. Nonlinear Sci. Numer. Simul.* 15 (2010) 2003–2016.
- [19] S.J. Liao, *Homotopy Analysis Method in Nonlinear Differential Equations*, Springer Berlin Heidelberg, Berlin, Heidelberg, 2012.